Research Article

Functional Information of a Driven Cellular Automaton

Hank Rainwater[1]

1. Independent researcher

For decades cellular automata (CA) simulations have proven versatile in modeling a wide range of complex natural phenomena due to their limited dimensionality and ability to allow adjustment of the small number of parameters that control self-organization. In this study, a model was designed that extends the self-organized phase of an automaton by keeping a single cell in a permanently (perennial) active state. After interacting with over 400,000 initial configurations of randomly placed standard automata cells surrounding the perennial cell, 351 unique and geometrically complex stable structures were created by the end state of evolution. These structures are analyzed with the goal of quantifying their complexity with Functional Information (FI) theory based on the degree of function of a structure within the CA environment using metrics of occurrence frequency quantifying information in bits. The expected selection bias inherent in CA is observed in this model and FI theory classifies each unique geometric structure according to its information content and eliminates observer bias frequently expressed as 'I know complexity when I see it' by replacing intuition with information.

Corresponding author: J. Hank Rainwater, rainwater.hank@gmail.com

1. Introduction

Quantifying complexity created by the emergence of self-organized structures in nature tax the analytical tools of science. In a seminal review by Rupe & Crutchfield[1] they comment that "After more than a century of concerted effort, physics still lacks basic principles of spontaneous self-organization." Identifying the control parameters is often where the hard work begins in understanding these systems where self-organization emerges during phase transitions – think of liquid water becoming ice – as the system reaches a critical point. This is why for decades cellular automata (CA) simulations have proven versatile in modeling a wide range of natural phenomena due to their limited dimensionality and ability to allow adjustment of the small number of parameters that control self-organization. Examples of CA applications include traffic flow[2], fluid dynamics[3], biology[4], urban planning[5], epidemiology[6], self-reproduction[7], artificial chemistry[8], quantum

 doi.org/10.32388/HX4713.3

mechanics[9] and autopoiesis and multicellularity[10]. With the increasingly important field of structural biology[11], where the chemical structures of life are studied, CA can also contribute to this domain of knowledge.

In previous research[12] I demonstrated how a modified version of Conway's Game of Life (GoL)[13], called perennial evolution (PE), can create stable and increasingly complex geometric patterns in phases of evolution from random initial configurations. This evolution, while non-Darwinian, is characteristic of complex systems with the ability to "dissipate energy or to maximize entropy production through patterning"[14]. PE is identified as *driven* because it continually injects order during evolution by keeping a CA cell or structure permanently active while maintaining and extending the system's dissipative action due to the physics of its state transition rule (STR)[15]. The structures created in PE display a selection bias and a variable chemistry-like reactivity, acting as an artificial chemistry. When these structures, considered as artificial molecules, and their history of formation are analyzed by the methods of functional information (FI) theory[16], a new understanding of self-organization and complexity is obtained for this driven CA. The goal of this work is to gather Insights from the application of FI to CA to provide new opportunities for modeling complex systems.

2. The Perennial Evolution Model

As an elaboration on my previous work, where several of the frequently occurring GoL still life patterns were modeled as artificial molecules, the current project considers how to first build artificial molecules from a single perennial cell. The model in this research is analogous to how the primordial elements created by stellar evolution in the early universe[17] eventually gave birth, over cosmological ages, to minerals that formed the geospheres of planets[18] in continuing phases of structure building[19].

2.1. Model Definition

As an extension of Conway's canonical GoL (CE), PE defines two types of active grid cells that can exist as shown in Figure 1, functioning as two-dimensional analogs of atoms that can bond and become structures representing *artificial* molecules. It is the construction process of this bonding and the resulting selection bias toward stable geometric patterns that is the focus of this research and not insights into the physics of creation of *real* molecules.

Figure 1. Atomic Components. Building blocks for construction of molecules in PE.

The bonding between the cells in Figure 1 is controlled by the physics of the STR that acts synchronously in discrete steps (*generations*) on all cells in the grid (*universe*) defined by the following rules:

1. Each inactive cell is defined as having the potential to become an active canonical cell and will become active if it has 3 active neighbors, otherwise it remains inactive.
2. A canonical cell that is active remains active during evolution if it has 2 or 3 active neighbors, otherwise it becomes inactive. This rule combined with rule 1 is often expressed using the nomenclature B3/S23 where 'B' signifies born and 'S' survive.
3. A perennial cell cannot be created by the STR but is manually introduced into the initial configuration of canonical cells prior to the beginning of a phase of evolution. A perennial cell is permanently active throughout all generations and can have as many active canonical neighbors at the 8 cardinal and intercardinal directions of the cell (the Moore neighborhood) as rules 1 and 2 will allow.
4. A collection of canonical cells bound to a single perennial cell resulting from the action of rules 1, 2 and 3 is considered a molecular object if it becomes a static geometric pattern during evolution and remains static until the universe reaches a quiescent end state. This end state occurs when the density of active cells in the evolving automaton reaches a constant or periodic value, but the pattern itself must be static. Also, the pattern must have bonds connecting all the cells, i.e., it must be a strict still life as defined by the GoL, consisting of only one 'island.'

Many familiar GoL still life will be created in PE because rules 1 and 2 are identical with the CE rules. However, patterns will also be created that cannot exist without a single perennial cell and these objects will have a special focus in the analysis of this research and referred to as PE molecules. An example of PE construction is shown in Figure 2 where the creation of still life objects occurs from a random initial collection of active CE cells and a single PE cell.

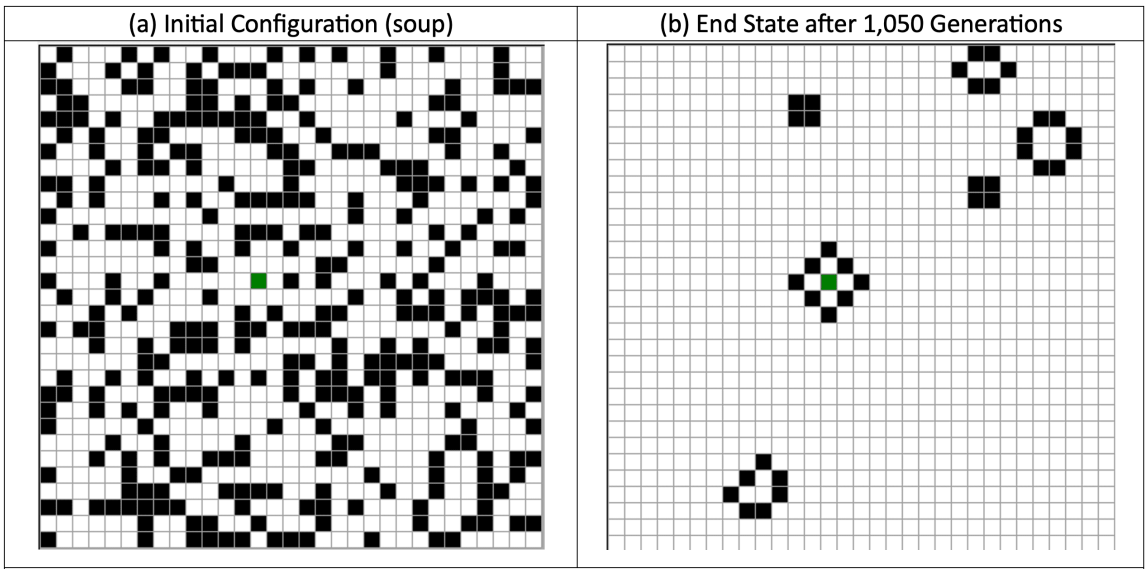

Figure 2. Perennial Evolution. A single perennial atom within a random soup of canonical atoms in (a) evolves after 1,050 generations to a static density in (b) creating a stable structure modeled as a molecule that could not exist without the perennial cell. This PE molecule at the center of the grid in (b) is named a 'Diamond'. Several other classic CE still life also appear at the end state. The universe size for this simulation is a 31 X 31 toroidal grid with an initial density of active cells in (a) of 35%.

With few exceptions it is common in PE for an embedded perennial cell to extend the number of generations for a random initial configuration of canonical cells to reach a static end state as compared with the same soup without the perennial cell. As an artificial chemistry this phenomenon can be viewed as the reactivity of the perennial cell – a type of catalytic effect – with the canonical cells. For example, in Figure 2, the soups in (a) without the perennial cell reached a static end state in 180 generations as compared to the 1,050 when a perennial cell is present. This catalytic effect – an extension of the region of dissipation during evolution where the rates of change per generation between active cells becoming inactive (death) and inactive cells becoming active (birth) are competing – is the region of self-organization that exhibits power law behavior[20]. These death/birth rates, called a dissipation factor (DF) can be measured and correlated with the number of generations that a soup requires to reach a static end state and will be discussed as an analytical tool applicable to the dynamics of pattern construction in a later section.

To emphasize the fact that PE created molecules are a *simulation* of a chemistry process, from this point forward molecules will be referred to as two-dimensional *patterns* that have a stable structure at the end state of evolution. The atoms will also be referred to as active *cells* to further clarify the nature of the model whose

primary purpose is to demonstrate self-organized complexity in a system of many locally interacting components.

2.2. Populating the Model with Data

Statistically significant ensembles of constructed patterns in PE are only revealed from evolution of a large set of initial state configurations (soups). Each soup contains a single perennial cell embedded among randomly positioned canonical cells. Each soup is unique and the position in the grid of a canonical cell is assigned by a random number generator each time a soup is created by the software designed for this project. A toroidal grid size of 31 rows and 31 columns with 961 cells for each soup has an active cell density of 35%, chosen because GoL dynamics are scale-invariant relative to grid size[21] and this density is in the range where self-organized criticality is optimal[22][23].

The total number of initial soups in the dataset for this project was 416,000 and each soup was set to evolve up to a maximum of 2,000,000 generations. Most of these soups (401,275) reached an equilibrium state prior to the maximum generation limit and those that did not reach equilibrium or were periodic were discarded from analysis. The initial soups were divided into 300 subsets to allow computation on a cluster of desktop computers.

The expected results of the dataset were the creation of patterns but 42.79% of the 401,275 soups did not produce any structure: the perennial cell remained unbound to canonical cells. However, 229,570 of the initial configurations, or 57.21%, produced a total of 351 stable patterns with 186 qualified as PE still life, unique from CE still life. The software developed for this project creates a signature for each pattern that defines its unique geometry by the number of cells per pattern as well as the number of bonds between the perennial cell and canonical cells. The patterns, as they were discovered during data population, are organized into families based on the number of canonical cells per pattern. In Figure 3 the number of patterns discovered per subset of data execution is presented, organized into families.

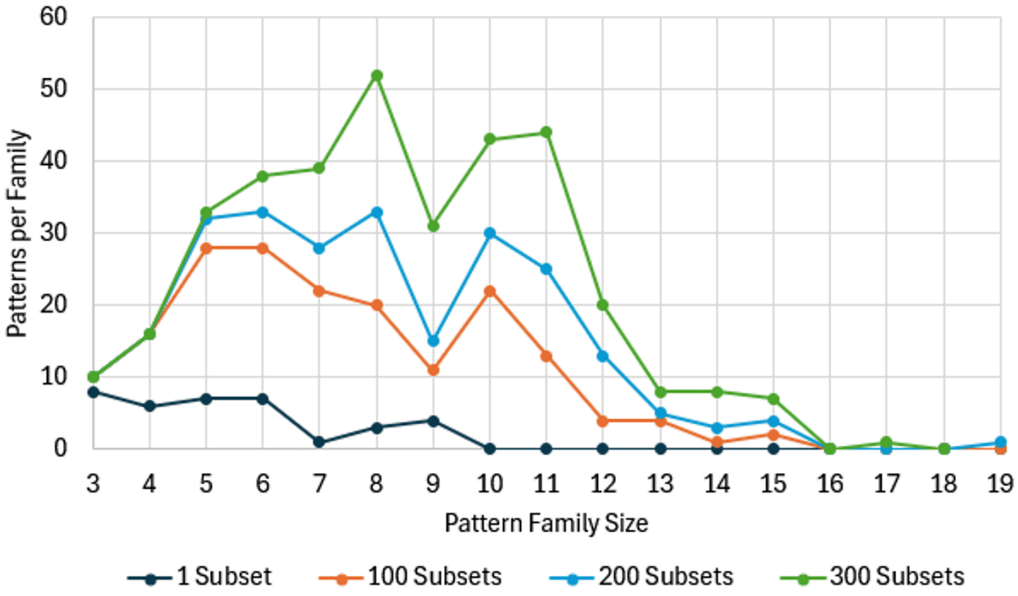

Figure 3. Discovery of Patterns. The first subset discovered 36 patterns, and the subsequent number discovered increased as additional subsets of soups were executed. The total number of subsets was 300, creating 351 total patterns. No patterns were discovered for family sizes 16 or 18 but are shown in the graph to highlight this fact.

The details of family patterns are discussed in the next section.

3. Pattern Phenomenology

The organizational scheme of patterns into families, based on the number of canonical cells per structure, was developed as limits to the variety of patterns that can exist within a family of a defined size were discovered. The smallest family size was 3 canonical cells bound to the single perennial cell and the largest was 19. A view of family statistics is shown in Figure 4.

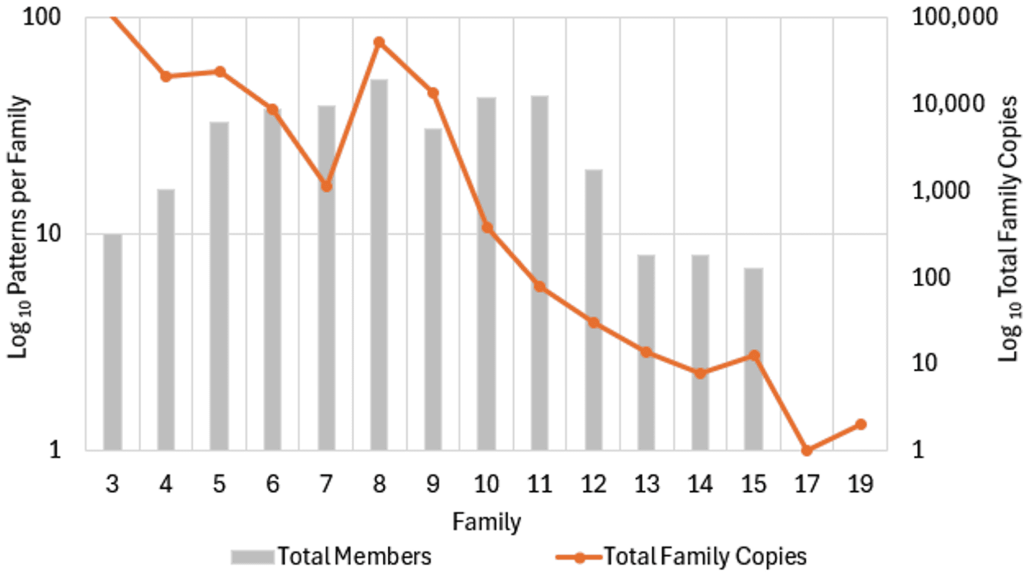

Figure 4. Family Statistics. Family 8 contains the PE pattern named 'Diamond' shown in Figure 2 (b) with over 53,000 copies Any correlation between the number of pattern copies per family versus the family size is not apparent in this data although there is a general falloff after family 9.

3.1. Minimum Pattern Size Limit

Patterns of less than three canonical cells cannot exist in PE nor in CE as illustrated in Figure 5.

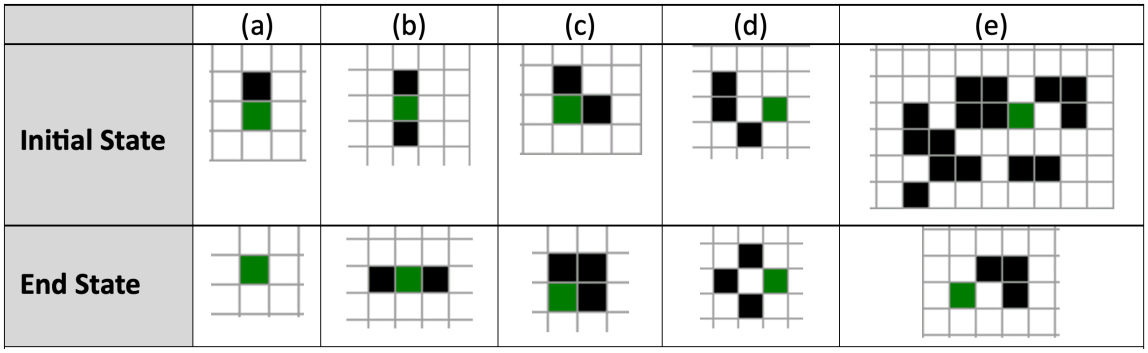

Figure 5. Minimum Pattern Size. In (a) the end state is not a valid still life pattern. In (b) this structure becomes the classic period 1 oscillator known as a Blinker in CE and is thus not stable nor qualifies as a pattern. In (c) a stable Block is formed and in (d) a stable Tub. The end state of (a) through (d) occurred in a single generation while in (e) the end state was reached in 1,278 generations from evolution with a random soup of canonical cells in which the perennial cell was embedded; the initial state shown is generation 1,277. (The Block and Tub were also created from random canonical soups with a single embedded perennial cell but shown here in a simplified form of creation.)

doi.org/10.32388/HX4713.3

The Block and Tub are part of a family identified as P_1C_3 since they contain 3 canonical cells bound to the single perennial cell, but they do not qualify as PE patterns since they can be created in CE. More on the PE pattern (e) in the next section.

3.2. Isomers in Families of Patterns

In addition to the minimum size of a pattern, many patterns in a family can appear in several orientations relative to the grid as two-dimensional spatial isomers (*stereoisomers*). For example, family P_1C_3 contains 8 stereoisomeric members as shown in Figure 6.

Molecular Structure						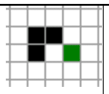	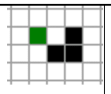	
Copies Created	217	211	209	204	202	201	197	181
Bond Location	NE	SW	SW	NE	SE	NW	SE	NW

Figure 6. Family P_1C_3 Stereoisomers. The perennial cell's bond location to a canonical cell varies among these patterns corresponding to the intercardinal directions of the Moore neighborhood. Rotation and/or reflection with respect to the XY-Plane of any one of these patterns demonstrates the structure's isometry. The total number of copies for all forms of this pattern is 1,622. This geometric form is unique to PE since it can't exist without the perennial cell.

Stereoisomers reveal that for a given family, e.g., P_1C_3, there is a limit to the number of unique patterns that can exist within a family of a specific number of canonical cells. If a pattern like those in Figure 6 is manually assembled where the first canonical cell is bound to the perennial cell's north binding location, the structure is not stable as seen in Figure 7.

Initial State	**Generation 1**	**Generation 2**	**Generation 3**	**.....**	**End State at 168 Generations**
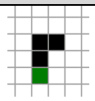	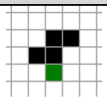	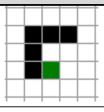	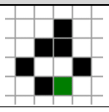	.....	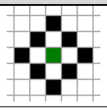

Figure 7. Nonstable Hypothetical P_1C_3 Object. A binding to the north of the perennial cell – as well as a binding to the east, south, or west – in the absence of any other canonical cells in the universe, results in the initial state evolving to a static configuration in 168 generations, but a stable pattern is created.

doi.org/10.32388/HX4713.3

The behavior of the evolution shown in Figure 7 results from the driven nature of PE where the presence of a perennial cell with only a few canonical cells injects order as the universe evolves. In this context the single PE cell acts as a catalysis within the CA universe of potential canonical cells, reacting at a rate governed by the STR. The position of the canonical cells bonded to the perennial cell in Figure 7 illustrates how critical geometry is to the final state of such a pattern. This sensitivity to position, a result of the STR that governs cell bonding, is demonstrated by the possible number of isometric forms that can exist for other families as seen in Figure 8.

Family	P_1C_4		P_1C_5			P_1C_6
Molecular Structure	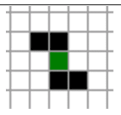		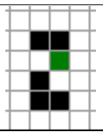	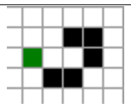	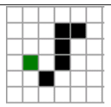	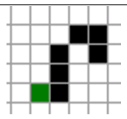
PE Atom?	True	True	False	True	True	False
Forms Detected	4	8	4	8	8	8

Figure 8. Isometric Patterns. In family P_1C_4 the two isomers complete the possible number of structures that can exist in this family (the Boat, discussed shortly, in its 4 forms are the remaining patterns in this family). The repeated appearance of 4 and 8 forms of structures is a function of the CA neighborhood with its 8 possible directions of bonding.

3.3. Selection Bias

Of the 351 patterns created from the 229,570 soups (see Section 2.2) in the dataset, 99% of the total are represented in Figure 9, ranked from left-to-right by their number of copies, and segregated by pattern type.

(a) Top Ranked PE Patterns								
Family	8	3	4	4	5	11	10	5
Pattern	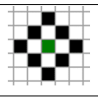	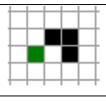	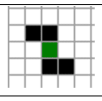	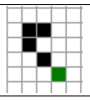	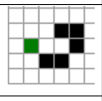	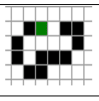	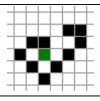	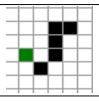
Name	Diamond	I3 -1	I4A -1	I4B - 1	I5A-1	I11A-1	I10A-1	I5B-1
Forms	1	8	4	8	8	7	7	8
Copies	53,337	1,622	460	288	186	37	33	33
(b) Top Ranked CE Patterns								
Family	3	4	9	5	3	5	6	5
Pattern			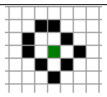					
Name	Block	Boat	Yacht*	Beehive	Tub	Barge	Loaf	Ship
Forms	1	4	4	2	1	2	4	2
Copies	94,219	20,056	13,811	11,674	10,696	8,717	8,022	3,708

Figure 9. Frequently Occurring Patterns. In (a) isomeric forms are named with a prefix of 'I' followed by their family number and rank per form, e.g., the image of pattern I3-1 had the largest number of copies among the 8 siblings and was discussed in Figure 6. In (b), several common GoL still life created by perennial evolution appear, but in a different rank than the GoL. For all patterns with more than one form, the number of copies is the total for all forms. *The 'Yacht', whose GoL name is 'Barge Siamese Loaf' is not used because I needed a shorter monicker for ease of reference. See Supplementary Data for a list of all 351 molecules in a spreadsheet format named All Molecules.xlsx.

While PE did produce several GoL top-ranked CE patterns, the ranking in PE can't be directly compared since the presence of a perennial cell changes the physics of evolution as well as the fact that the GoL ranking environment (LifeWiki) uses a different grid size and type as well as a different initial soup density than PE. Regarding the PE patterns, they are unique and demonstrate a different physics in operation compared with the GoL.

4. Functional Information Theory for Perennial Evolution

The phenomenology presented in the previous section illustrated the selection bias differences between PE and CE: quantifying these differences with FI theory is the task of this section. In Hazen's study on complexity in patterning systems[24] FI is defined as a "degree of function (E_X) [that is] a quantitative measure of a configuration's ability to perform the function X." In PE, this function is the system's ability to create stable patterns, and the "quantitative measure" is given by the formula:

$$I(E_X) = -\log_2[F(E_X)] \quad (1)$$

In the context of PE, the "degree of function (E_X)" is a measure of the action performed by the STR to form a stable pattern[25] with ≥ 3 active canonical cells with a single perennial cell as demonstrated above in Figure 5, while $F(E_X)$ is the "fraction of all possible configurations of the system that achieves a degree of function $\geq E_X$" and is defined in this research as the Functional Information Detection Ratio (FIDR) as follows...

$$\mathrm{FIDR} = \mathrm{N}_{\mathrm{copies}} \ / \ \mathrm{N}_{\mathrm{soups}} \tag{2}$$

where...

- N_{copies} = the number of copies of a specific pattern
- N_{soups} = 401,275 i.e., the total number of simulations producing all patterns (Figure 3).

FIDR thus defines a measure of the probability of a pattern's occurrence within the evolving system and Equation 1 quantifies this value in bits.

The 401,275 configurations (from the initial 300 subsets of soups) are the "all possible configurations" where each configuration could result in the creation of a pattern, even though only 229,570 configurations did create a pattern and achieve the defined degree of function. However, FI considers the larger value discussed in Section 3 of 401,275 soups as representative of the state of knowledge about the system prior to any evolutions of the automaton, that is, all configurations are initially equally likely to produce patterns of the defined degree of function because the probability distribution of the system is uniform – and unknown – prior to any evolutions being performed[26]. Once evolution begins, information about the system increases with the value of $I(E_X)$ in bits quantifying this new information. It is also important to note that the functional information of a pattern is not the property of a pattern in isolation, "but of the ensemble of all possible sequences, ranked by activity"[16][27]. This activity of the environment is shown in Figure 10 where the FI and FIDR values for all 351 patterns are displayed.

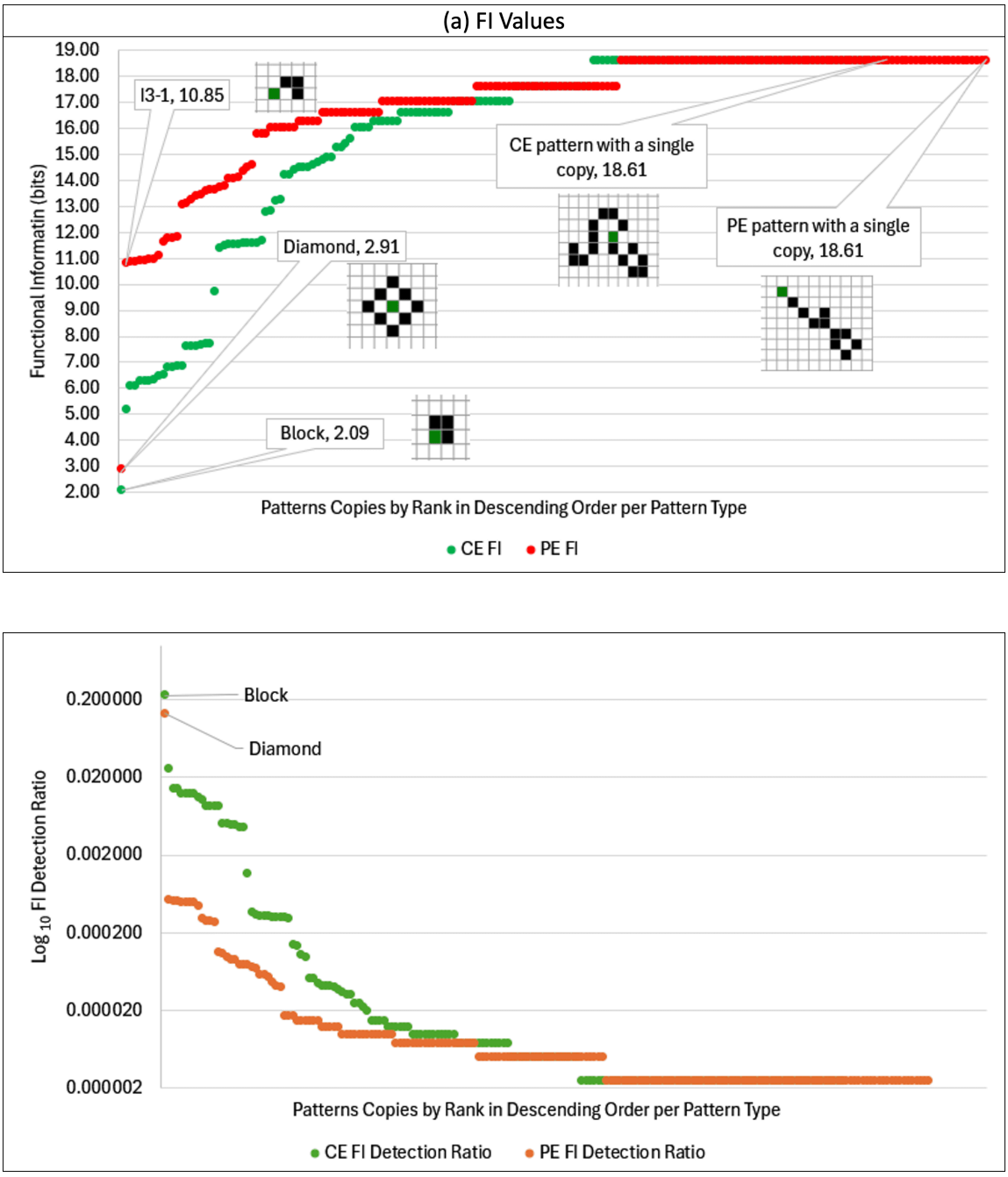

Figure 10. FI and FIDR Values for all Patterns. An inverse relation is shown between (a) and (b): as the FI values in bits increase, the FIDR values decrease.

While the two images of patterns with an FI value of 18.61 bits in Figure 10 (a) offer an intuitive picture of complexity along the lines of the time-worn saying, "I know it when I see it," the degree of function quantified by FI replaces intuition with information. The concept that a function can be equated with the stability of a

doi.org/10.32388/HX4713.3

geometric object has proven useful in other work[28] and the next section explores the relationship between the physics of pattern construction and complexity.

5. Analysis of Pattern Construction

Using the insights from the previous section where complexity is quantified by FI theory, several aspects of pattern creation in PE are analyzed in this section: construction dynamics, the role of the number of bonds between the PE cell and canonical cells, and motifs in patterns will be examined. Keep in mind that complexity is defined in this work by a theory where frequency of occurrence (FIDR) and information in bits (FI) have an inverse relationship.

5.1. Construction Dynamics

How does the presence of the perennial cell effect construction of patterns? An explanation is as follows: a CA with deterministic rules but an evolution contingent on the interaction of every cell in the CA universe with each of its eight neighbors at each discrete generation of the evolution demonstrates a particular type of contingent behavior. This contingency is described in the context of paleontological history as "...a thing unto itself, not the titration of determinism by randomness"[29]. In this view of biology, evolution is driven by random genetic mutations with natural selection acting as a *filter* allowing reproductively successful mutations to survive. In the context of a driven CA, the single PE cell also functions as a type of filter by acting as an *attractor* of canonical cells, forming stable structures in the region of the CA universe in which it is located. This attraction results in changing the dynamics of construction in the area around the PE cell while the dynamics in the rest of the universe follow the canonical GoL rules as stated in the model definition of Section 2.

An example of this attractive effect of a perennial cell is demonstrated during the construction of the Block, ranked #1 in both the Gol and PE, the least complex according to FI theory at 2.09 bits, occurring 94,219 times in the CA universe and having the largest FIDR value of all the patterns. All 94,219 instances of its creation are shown in a histogram in Figure 11 displaying the number of generations of each Block's formation prior to the end state of the soup. These generational values are named Construction Steps (CS) and are not equal to the number of generations for a soup to reach its quiescent end state.

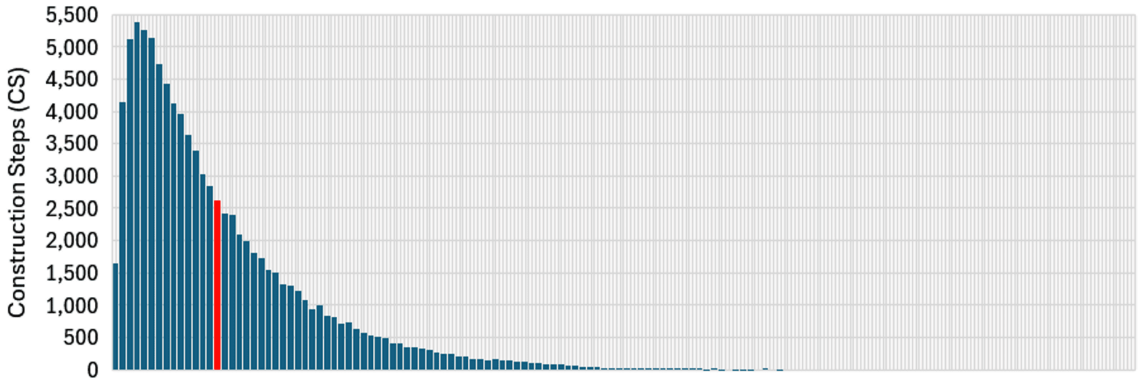

Figure 11. Block's CS Values. The minimum CS is 4 generations, the maximum 7,176 with an average of 749.22 as shown by the red column in the histogram. The standard deviation of the CS values is 678.38 generations. At each CS value, the Block is formed and remains stable until the end state of the soup is reached. The histogram's horizontal axis contains bins of size 52 but the bin ranges are not shown due to space limitations on the page.

The range of values in this histogram – its highly skewed long tail distribution – demonstrates the contingency described above and is common for the frequently occurring patterns created in PE as seen in Figure 9. This non-normal distribution is a signature of the activity of a power law during the self-organizing phase of pattern construction as seen for all 94,219 evolutions of the Block with the potential of black swan events[30] occurring. See the Appendix for more detail on this distribution of values and the large variations that occur.

In keeping with the design of FI theory, analysis must treat the entire ensemble of events during pattern construction. This means that the mathematically determined average CS value of a distribution such as the Block in Figure 11 is not an expected typical value. However, using the minimum and maximum CS values for the Block will illustrate the dynamics of the construction process over the range of values in which the Block was created. These values were measured for the Block and the other 350 patterns discovered in the dataset and can be viewed in Supplementary Data.

To drill down on the details of this construction process, a heat map designed for this project's software to track the state transition (active-to-inactive or inactive-to-active) of each cell in the CA universe at each generation of evolution and measures the percentage of evolutionary time a cell is active, illustrating the attractive function of the PE cell when a Block is created as shown in the next several figures.

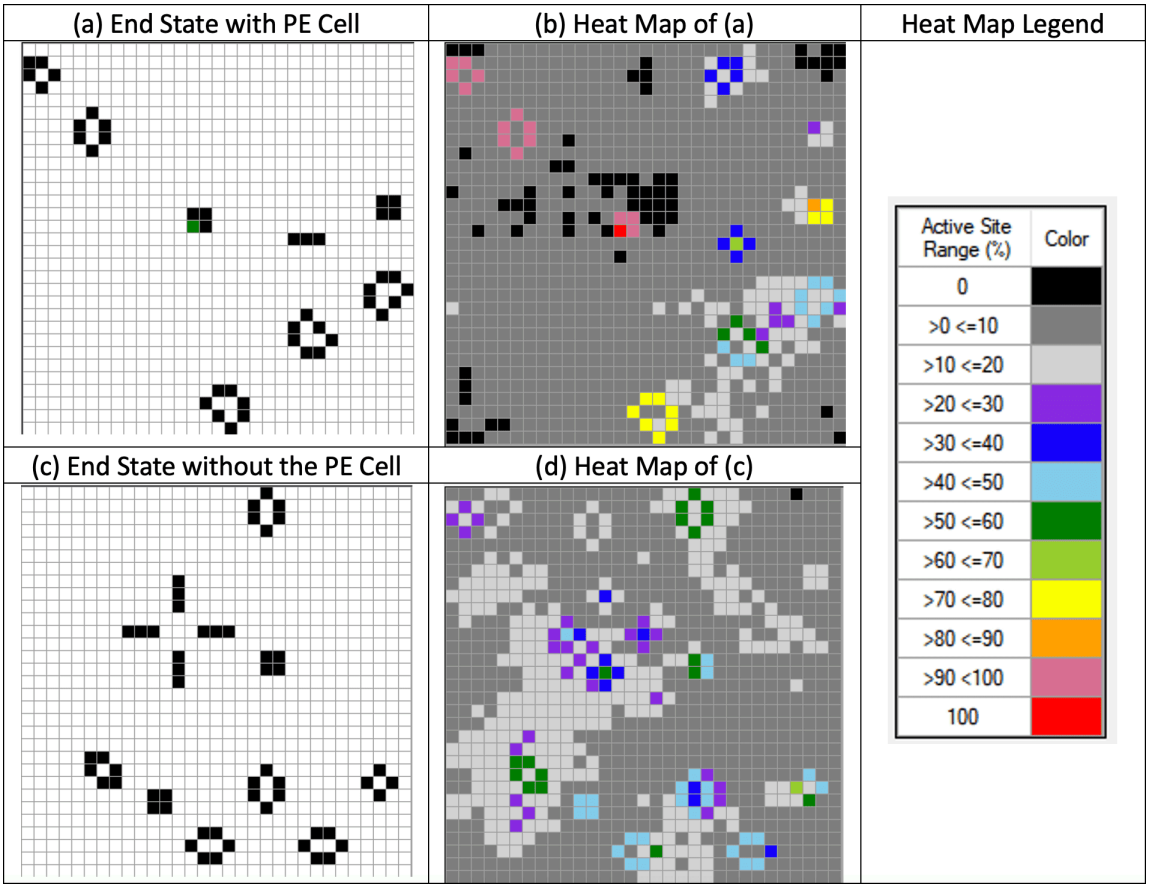

Figure 12. PE Block's Minimum Construction Steps. In (a) the Block formed in 4 generations and remained stable until the end state of 200 generations. The PE cell in (a) was active during all generations and thus its activity as measured by the heat map was 100%. The three canonical cells that are part of the PE Block were also active in the a range of over 90% to slightly less than 100%. The cells black in color near the Block in the heat map are evidence that once the Block formed at generation 4, it was somewhat isolated from the interactions occuring elsewhere in the universe. In (c) the same soup as (a) *without* the PE cell created a different pattern of structures after 350 generations without any cells having activity as high as those in (b).

A closer look at the region of the grid around the perennial cell in Figure 12 is shown in Figure 13 demonstrating the difference in dynamics between PE and CE.

doi.org/10.32388/HX4713.3

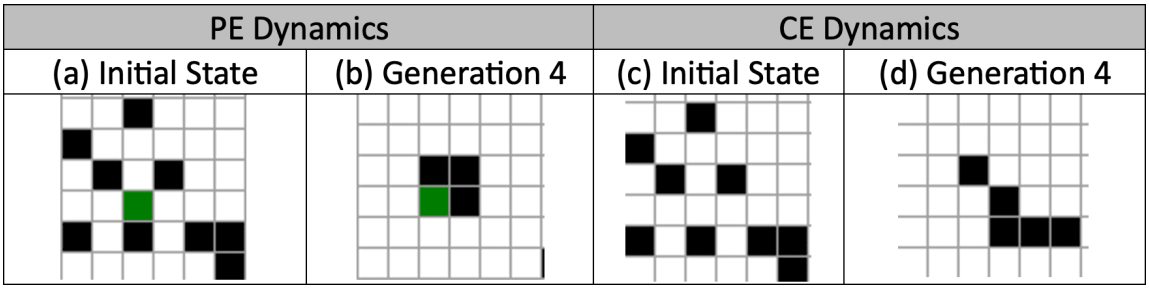

Figure 13. PE vs CE Dynamics. In (a) only the region in the soup around the PE cell is shown and the Block is constructed at generation 4 in (b) and remains stable until the end state. The same soup in (c) without the PE cell has a different evolution as seen in (d) after 4 generations and continues to evolve until the end state shown in Figure 12 (c).

The Block being constructed at the maximum number of construction steps is shown next.

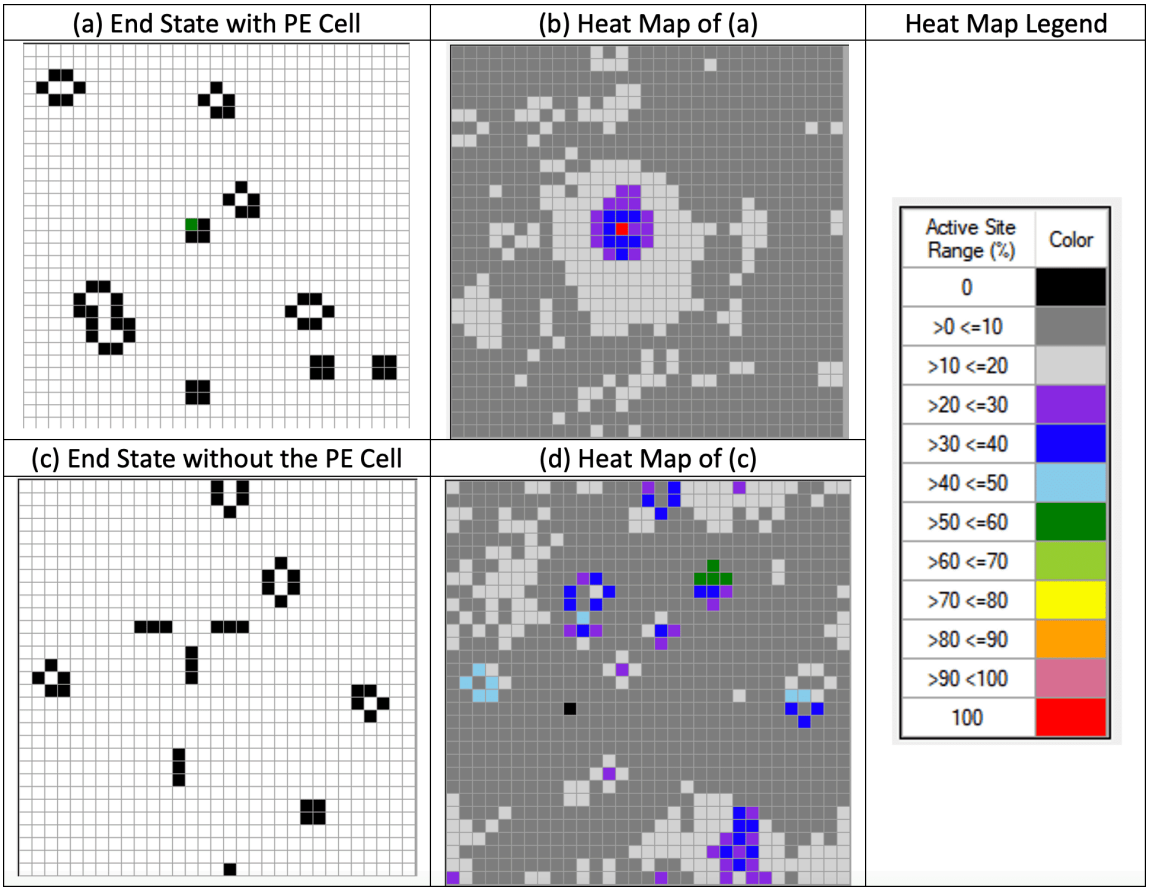

Figure 14. PE Block's Maximum Construction Steps. In (a) the end state occurred after 7,176 generations with the the PE cell's attractive effect in (b) more obvious than that shown in Figure 12. In (c) the end state was reached in 450 generations without the PE cell in the soup.

doi.org/10.32388/HX4713.3

The effect of a single PE cell in Figures 12, 13 & 14 – both its presence and absence – demonstrates that PE contingency is "a thing unto itself" where the end state is unpredictable, but the attractive effect of a PE cell is clear, changing the dynamics of self-organization around the PE cell as compared with the rest of the universe. A more dramatic example of dynamic differences is given in Figure 15 for the Diamond, the most frequently occurring PE pattern.

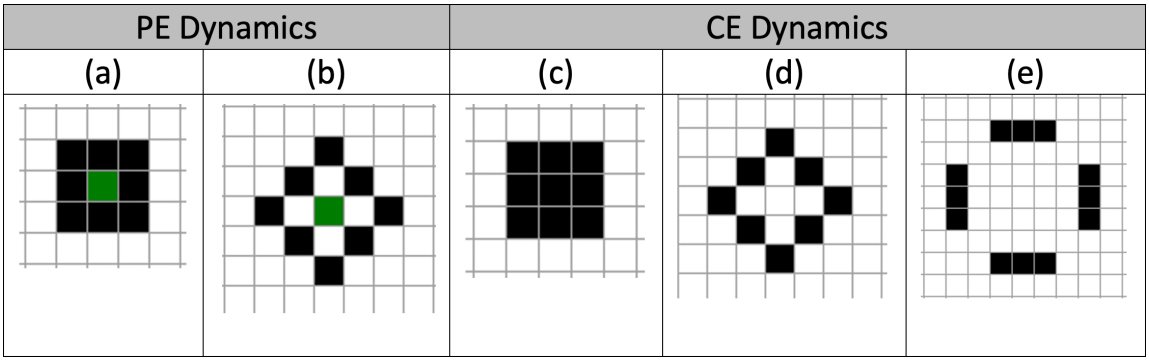

Figure 15. Construction Dynamics. A possible initial random state of canonical cells around the region of the PE cell in (a) creates a PE Diamond in a single generation of evolution in (b). Note that its actual minimum CS was measured at 13 generations, so this example is hypothetical. In (c) a similar initial state as in (a) without the PE cell creates the unstable structure in one generation in (d) that becomes a GoL oscillator in (e) after 5 generations known as a 'Traffic Light'.

In terms of occurrence frequency, the Block and Diamond could be discussed in Darwinian terminology as 'survival of the least complex' where survival is measured as the degree of abundance. The other PE-generated patterns also survived and ranked according to their FIDR derived complexity. This explanation is, of course, given after the simulations have been performed since the contingent nature of CA evolution does not allow rank to be predicted analytically prior to evolution. Thus, the concept of rank is *a posteriori* like 'fitness' in biological evolution[31].

5.2. Perennial Cell Binding

The various geometric forms of patterns and their relationship to the binding strength of the PE cell are considered in this section. In this context, *strength* is a function of the number of bonds the single perennial cell has to canonical cells. This binding, of course, is due to the STR where it can have as many active canonical neighbor cells as the B3/S23 rule will allow and is an analogy for valency. How the number of bonds affects a pattern's geometric configuration and subsequent FI value is summarized in Table 1.

PE Cell Bonds	Pattern Type	Number of Patterns	Range of FI Values in Bits	Least Complex Example	Most Complex Example
1	PE	79	10.85 to 18.61	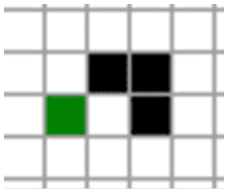	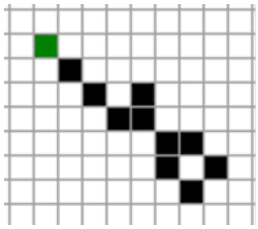
2	CE	78	5.23 to 18.61	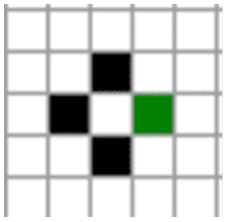	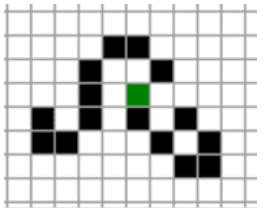
3	CE	87	2.09 to 18.61		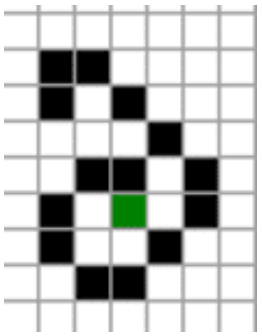
4	PE	85	2.91 to 18.61	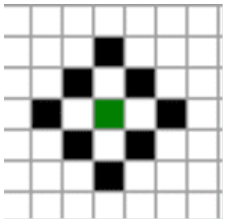	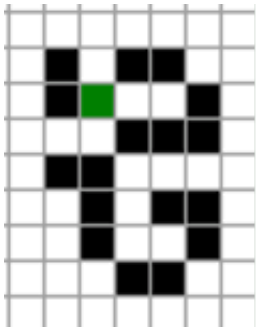

doi.org/10.32388/HX4713.3

PE Cell Bonds	Pattern Type	Number of Patterns	Range of FI Values in Bits	Least Complex Example	Most Complex Example
5	PE	21	17.03 to 18.61	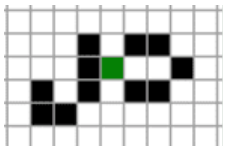	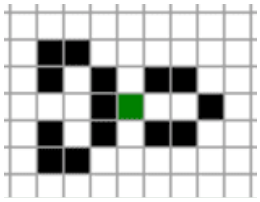
6	PE	1	18.61	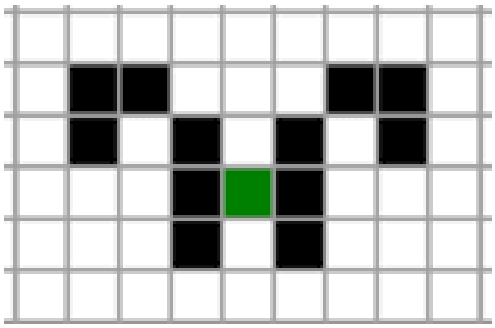	

Table 1. Complexity and PE Cell Bonds. All bond values produced patterns with the largest FI values, but the bond values 5 & 6 only were able to produce PE patterns of high complexity compared with the lower bond values. Complexity in this table is quantified by the functional information value in bits.

All the patterns with 1, 4, 5 or 6 bonds could not be created by the GoL and thus the perennial cell's binding strength is the contributing factor to their complexity as defined by functional information theory. The 79 PE patterns that have only a single bond to their PE cell are prime examples of this fact.

5.3. Construction Motifs

You may have noticed in the previous section that some of the patterns contained as part of their structure several of the frequently occurring patterns such as a Boat and Beehive. One might imagine that during evolution these frequent patterns were first created and then several other cells added almost as an afterthought. Your imagination would not be leading you astray in this case. In addition to this observation, you no doubt noticed how frequently diagonal cells of three or more cells appear in a structure, for instance with the

doi.org/10.32388/HX4713.3

Loaf, Yacht, and Barge in CE still life as well as the Diamond, a PE-only pattern. Also, a 'hook' like that shown below in Figure 16 often appears in some patterns.

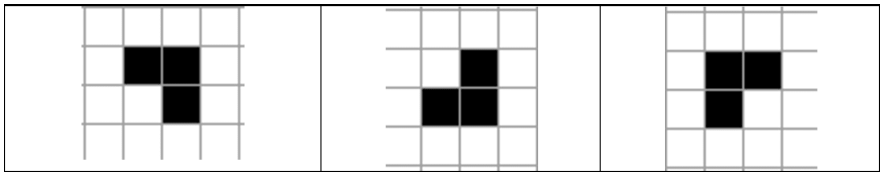

Figure 16. A Hook Motif in Several Orientations. Sometimes a hook may be extended in one direction and referred to as a 'tail'.

Space in this manuscript has a limit and thus more images exemplifying this motif effect can't be shown here; I encourage the reader to open the Supplementary Data spreadsheet and view many of the more complex and thus less frequently occurring patterns. There you will see a Tub with a hook as well as many other instances of long diagonal cells, Beehives with ornamentation and in one rare instance a Block connected to a Ship.

The reason these motifs are a factor during construction is that the physics of PE does indeed create frequently occurring patterns during evolution to an end state. For example, during the creation of a Block, in the instance of its maximum CS value (Figure 14), 7,176 generations occurred before the Block was formed and remained unchanged until the end state occurred at 7,250 generations. During this long period of evolution, the CA produced several patterns that briefly remained stable before continuing evolution changed the universe's state as seen in Figure 17.

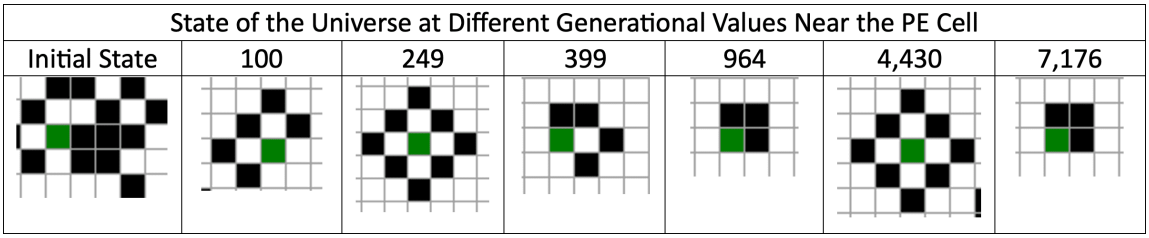

Figure 17. Several Examples of the Block's Metamorphosis. The initial state became a Barge, Diamond, Boat, Block, and again a Diamond before reaching its final form at generation 7,176, unchanged until the end state of evolution at 7,250 generations.

doi.org/10.32388/HX4713.3

6. Discussion and Outlook

Perennial evolution drives a cellular automaton to longer phases of self-organization due to the catalytic and attractive effect of a permanently active cell. The creation in this CA of unique geometric patterns – two-dimensional analogues of molecules – resulted from the action of the perennial cell. While FI theory quantified the complexity of patterns, it did not illuminate all aspects of PE evolution. For example, symmetry is a feature of patterns in this research with the Block and Diamond as the two most frequently occurring patterns exhibiting rotational symmetry. In addition, many isometric forms with high complexity are explained more accurately by the STR in two dimensions due to the unique bonding characteristics of the perennial cell for those PE patterns that can't exist in the canonical GoL.

In work not yet reported, I created an additional 100 subsets of data that increased the total initial configurations by 96,543. The result of this increase did not change the relative occurrence frequency of the reported patterns described in this work but did create 35 new patterns. Of these 35 new discoveries 18 were very similar to what had been previously created with a single PE bond; some were simply new isometric forms of previous patterns. Thus, the capacity for diversity in perennial evolution appears limited, even for those patterns with only a single bond creating stability. While the FI values of patterns will increase with additional subsets of initial configurations, it is not certain that their diversity increases despite an increase in complexity as quantified by functional information theory.

An example of future ideas that could be explored with the techniques developed in this research, consider two patterns as analogues of primordial minerals that bond with each other. This would be analogous to the way minerals become more complex[25] over long periods of geological time during which thermodynamic and gravimetric churning introduce phase changes[32]. These phase changes could be represented as the conversion of primordial mineral patterns to a fully perennial form as shown in Figure 18 and allow the patterns to interact *without* any soup of canonical cells, forming new stable structures.

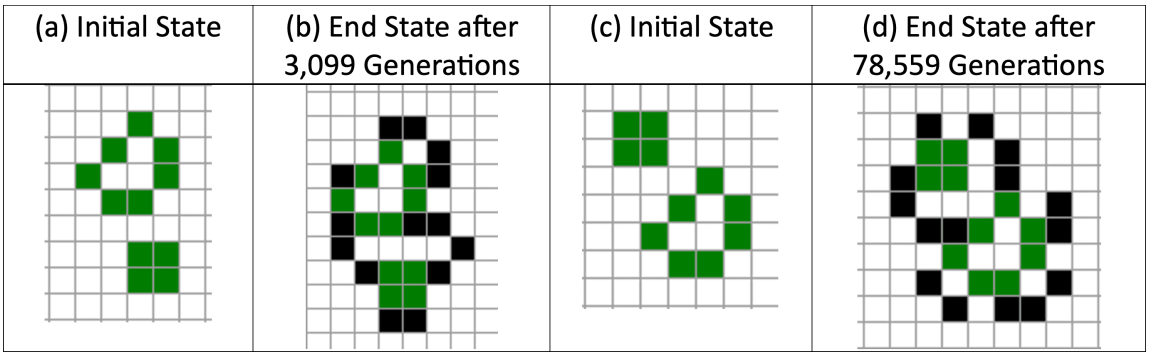

Figure 18. A Loaf and Block as Interacting Patterns. The relative location of the two patterns shown in (a) vs (c) results in different end state structures as well as differences in the length of self-organized construction as measured in generations.

This project's model has demonstrated one technique of using cellular automata to quantify complexity, and future possibilities remain to be explored. Good hunting to all those who share in this quest.

Appendix: Significance of a Power Law for the Block's Creation

A scatter plot of all 94,219 soups that created a Block is shown in Figure A1 that demonstrates the power law behavior of the self-organizing phase of evolution of these soups. This power law is characterized by a dissipation factor (DF) defined as the difference in the rate per generation of active cells becoming inactive versus inactive cells becoming active over the course of a universe's evolution to a static end state[12].

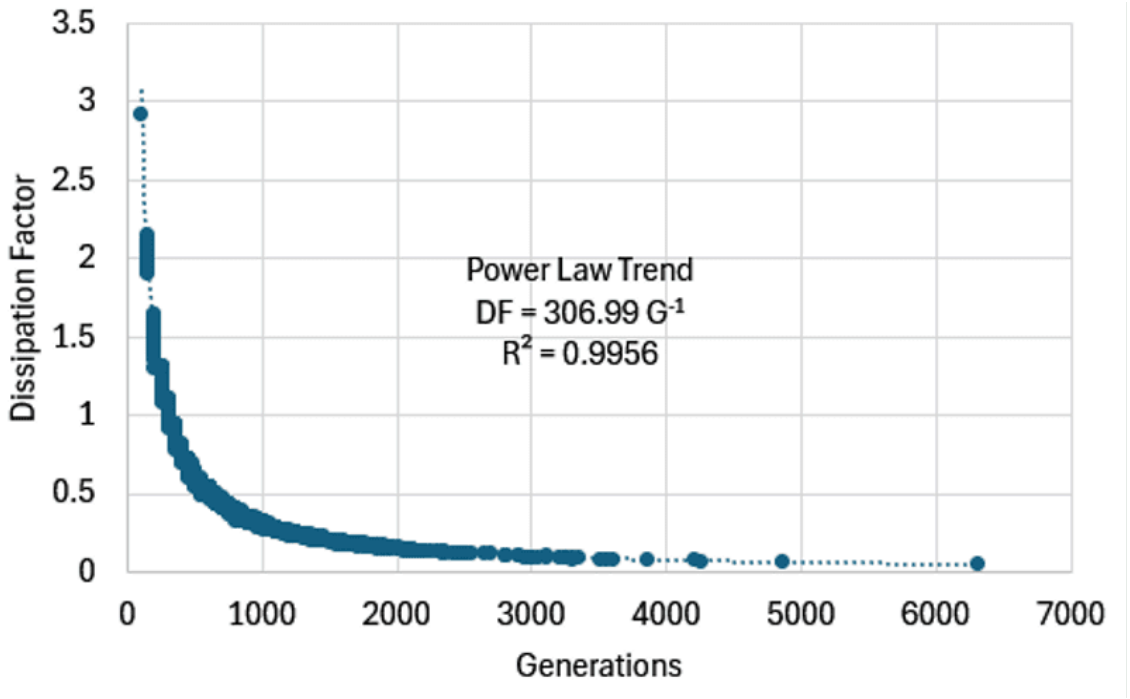

Figure A1. Correlation of Dissipation Factor and Generations. The generations (G) are the value of the end state of each soup. The power law trend constant (306.99) is only valid for a grid of size 31 X31[12].

The DF for each soup varies as a function of the number of generations. In most cases, as seen in this research, it was noted that a soup with a perennial cell extends the number of generations required for a soup to reach an end state as compared with the same soup without a perennial cell. The effect of the perennial cell can be measured using the dissipation factor by calculating the DF difference between soups with a perennial cell and the same soups without a perennial cell. This difference is called the Differential Dissipation Factor (DDF) defined as follows:

$$\mathrm{DDF}(\%) = ((\mathrm{DF}_{\mathrm{SOUP}} - \mathrm{DF}_{\mathrm{PERENNIAL\ CELL\ +\ SOUP}}) \,/\, |\mathrm{DF}_{\mathrm{SOUP}}|) \ * \ 100$$

For the Block, the DDF = 7.4% measured from a 1,000-soup subset of the 94,219 total soups. This DDF value quantifies the dynamics discussed in the heat map displays where the perennial cell raises the overall active cell percentage compared with the same soup without the perennial cell.

Related to the above discussion are the variations in the CS values for patterns. In Table A1 the frequently occurring patterns (Figure 9 in the text) are listed by their number of copies for each form of the pattern. The Diamond is included in this list since it was the second most frequent pattern discovered.

Pattern	Detections	FIDR	Min CS	Avg CS	Max CS
Block	94,219	0.23480	4	749.22	7,176
Diamond	53,337	0.13292	13	761.61	9,075
Tub	10,696	0.02666	7	746.32	6,580
Beehive 1	5,839	0.01455	9	751.77	5,677
Beehive 2	5,835	0.01454	12	755.65	6,043
Boat 1	5,055	0.01260	10	738.47	7,626
Boat 2	5,031	0.01254	8	729.91	7,157
Boat 3	5,010	0.01249	7	748.76	6,180
Boat 4	4,960	0.01236	10	752.95	6,104
Barge 1	4,460	0.01111	16	739.44	6,156
Barge 2	4,257	0.01061	13	752.47	5,200
Yacht-1	3,480	0.00867	15	757.82	5,957
Yacht-2	3,474	0.00866	19	734.44	4,779
Yacht-3	3,432	0.00855	19	745.89	5,732
Yacht-4	3,425	0.00854	20	768.49	4,850
Loaf 1	2,042	0.00509	11	751.93	5,757
Loaf 2	2,038	0.00508	27	753.90	5,293
Loaf 3	1,979	0.00493	24	755.31	6,145
Loaf 4	1,963	0.00489	9	721.81	5,885
Ship 1	1,855	0.00462	18	755.12	6,218
Ship 2	1,853	0.00462	15	770.63	6,157

Table A1. FIDR and CS Values for the Frequently Occurring Patterns. As the number of copies decreases the FIDR decreases as expected according to Equation 2. None of the CS values show any correlation with the FIDR values.

The CS average of the patterns in Table A1 is 750 ± 12 generations that includes 21 CE patterns and 1 PE pattern.

By comparison, the average CS value of all CE patterns was 782 ± 479 generations while all PE patterns had an average CS of 755 ± 440 generations. Due to the large variations associated with the average CS values for all CE and PE patterns, no significance can be attributed to the differences between the CE and PE averages because they are not expected, typical values due to the long-tail distribution of values seen with the Block, a feature common for all the CS values for all patterns. These differences are yet another aspect of contingency in CA evolution that derives from the power law behavior during self-organization. A breakdown of the large standard deviations (STD) noted above as a function of the number of copies of a pattern is shown in Table A2.

Pattern Rank	Number of Copies	Average CS STD
1 to 21	Greater than 1,000	12
22 to 44	100 to less than 1,000	57
45 to 208	2 to less than 100	346
209 to 351	1 copy	616

Table A2. Increase in Average CS Standard Deviation with decrease in Pattern Copies.

As seen in this table, the number of copies of a pattern directly affects the variations within the distribution of values where black swan events are common with power-law behavior.

Statements and Declarations

Funding

No specific funding was received for this work.

Potential competing interests

No potential competing interests to declare.

Data and Code Availability

The software and source code developed for this project are open-source and available for download via GitHub.

Use of AI in Research

Google's Gemini large language model was used to discover peer-reviewed resources for a portion of this research.

Acknowledgements

The author thanks Qeios reviewers Dr. Al-Dabbagh, Serge Dolgikh, Fabrizio Browen, and Szymon Lukaszyk for helpful comments, insights and analysis.

References

1. ^*Rupe A, Crutchfield JP (2024). "On Principles of Emergent Organization." Phys Rep. **1071**:1–47. doi:10.1016/j.physrep.2024.04.001.*
2. ^*Deng X, Shao Y, Song J, Wu H (2022). "Traffic Flow Simulation of Modified Cellular Automata Model Based on Producer-Consumer Algorithm." PeerJ Comput Sci. **8**:e1102. doi:10.7717/peerj-cs.1102. S2CID 252417533.*
3. ^*Frisch U, Hasslacher B, Pomeau Y (1986). "Lattice-Gas Automata for the Navier-Stokes Equation." Phys Rev Lett. **56**(14):1505. https://journals.aps.org/prl/pdf/10.1103/PhysRevLett.56.1505.*
4. ^*Graner F, Glazier JA (1992). "Simulation of Biological Cell Sorting Using a Two-Dimensional Extended Potts Model." Phys Rev Lett. **69**(13):2013. doi:10.1103/PhysRevLett.69.2013.*
5. ^*Batty M (2007). Cities and Complexity: Understanding Cities with Cellular Automata, Agent-Based Models, and Fractals. The MIT press. https://dl.acm.org/doi/abs/10.5555/1543541.*
6. ^*White SH, Del Rey AM, Sánchez GR (2007). "Modeling Epidemics Using Cellular Automata." Appl Math Comput. **186**(1):193–202. doi:10.1016/j.amc.2006.06.126.*
7. ^*Langton CG (1984). "Self-Reproduction in Cellular Automata." Physica D: Nonlinear Phenomena. **10**(1-2):135–144. doi:10.1016/0167-2789(84)90256-2.*
8. ^*Hutton TJ (2002). "Evolvable Self-Replicating Molecules in an Artificial Chemistry." Artif Life. **8**(4):341–356. doi:10.1162/106454602321202417.*
9. ^*Flitney AP, Abbott D (2010). "Towards a Quantum Game of Life." In Game of Life Cellular Automata. London: Springer London. pp. 465-486. https://www.researchgate.net/profile/Adrian-Flitney/publication/236109736_Towards_a_Quantum_Game_of_Life/links/55666d3208aec22682ff1b0f/Towards-a-Quantum-Game-of-Life.pdf.*
10. ^*Turney PD (2021). "Evolution of Autopoiesis and Multicellularity in the Game of Life." Artif Life. **27**(1):26–43. doi:10.1162/artl_a_00334.*
11. ^*Curry S (2015). "Structural Biology: A Century-Long Journey into an Unseen World." Interdiscip Sci Rev. **40**(3):308–328. doi:10.1179/0308018815Z.000000000120.*

12. ^a, b, cRainwater JH (2024). "Self-Organization and Phase Transitions in Driven Cellular Automata." Artif Life. **30** (3):302–322. doi:10.1162/artl_a_00437.
13. ^Gardner M (1970). "Mathematical Games." Sci Am. **223**(4):120–123. doi:10.1038/scientificamerican1070-120.
14. ^Hazen RM, Griffin PL, Carothers JM, Szostak JW (2007). "Functional Information and the Emergence of Biocomplexity." Proc Natl Acad Sci U S A. **104**(suppl_1):8574–8581. doi:10.1073/pnas.0701744104.
15. ^Beer RD (2020). "An Investigation into the Origin of Autopoiesis." Artif Life. **26**(1):5–22. doi:10.1162/artl_a_00307.
16. ^a, bSzostak JW (2003). "Functional Information: Molecular Messages." Nature. **423**(6941):689–689. doi:10.1038/423689a.
17. ^Johnson JA, Fields BD, Thompson TA (2020). "The Origin of the Elements: A Century of Progress." Phil Trans R Soc A. **378**(2180):20190301. doi:10.1098/rsta.2019.0301.
18. ^Hazen R, Morison S (2020). "An Evolutionary System of Mineralogy. Part I: Stellar Mineralogy (>13 to 4.6 Ga)." Am Mineral. **105**(5):627–651. doi:10.2138/am-2020-7173.
19. ^Smith E, Morowitz HJ (2016). The Origin and Nature of Life on Earth: The Emergence of the Fourth Geosphere. Cambridge: Cambridge University Press.
20. ^Bak P, Chen K, Creutz M (1989). "Self-Organized Criticality in the Game of Life." Nature. **342**(6251):780–782. https://www.nature.com/articles/342780a0.pdf.
21. ^Peña E, Sayama H (2021). "Life Worth Mentioning: Complexity in Life-Like Cellular Automata." Artif Life. **27**(2):105–112. doi:10.1162/artl_a_00348.
22. ^Reia SM, Kinouchi O (2014). "Conway's Game of Life Is a Near-Critical Metastable State in the Multiverse of Cellular Automata." Phys Rev E. **89**(5):052123. doi:10.1103/PhysRevE.89.052123.
23. ^Garcia JBC, Gomes MAF, Jyh TI, Ren TI, Sales TRM (1993). "Nonlinear Dynamics of the Cellular-Automaton "Game of Life"." Phys Rev E. **48**(5):3345. doi:10.1103/PhysRevE.48.3345.
24. ^Hazen RM (2009). "The Emergence of Patterning in Life's Origin and Evolution." Int J Dev Biol. **53**(5-6):683–692. https://www.researchgate.net/profile/Robert-Hazen/publication/26321936_The_emergence_of_patterning_in_life's_origin_and_evolution/links/00b7d531f32666b39d000000/The-emergence-of-patterning-in-lifes-origin-and-evolution.pdf.
25. ^a, bHazen RM, Wong ML (2024). "Open-Ended Versus Bounded Evolution: Mineral Evolution as a Case Study." Pnas Nexus. **3**(7):page 248. doi:10.1093/pnasnexus/pgae248.
26. ^Adami C (2016). "What Is Information?" Phil Trans R Soc A. **374**(2063):20150230. doi:10.1098/rsta.2015.0230.
27. ^Adami C, Cerf NJ (2000). "Physical Complexity of Symbolic Sequences." Physica D: Nonlinear Phenomena. **137**(1-2):62–69. https://www.sciencedirect.com/science/article/abs/pii/S0167278999001797?via%3Dihub.

28. ^Wong ML, Cleland CE, Arend D Jr, Bartlett S, Cleaves HJ, Demarest H, Prabhu A, Lunine JI, Hazen RM (2023). "On the Roles of Function and Selection in Evolving Systems." Proc Natl Acad Sci U S A. **120**(43):e2310223120. doi:10.1073/pnas.2310223120.
29. ^Gould SJ (1989). Wonderful Life: The Burgess Shale and the Nature of History. New York, NY: W. W. Norton & Co.
30. ^Sornette D (2009). "Dragon-Kings, Black Swans and the Prediction of Crises." arXiv preprint. https://doi.org/10.48550/arXiv.0907.4290.
31. ^Thurner S, Hanel R, Klimek P (2010). "Physics of Evolution: Selection Without Fitness." Physica A. **389**(4):747–753. doi:10.1016/j.physa.2009.10.030.
32. ^Schwartzman DW, Shore SN, Volk T, McMenamin M (1994). "Self-Organization of the Earth's Biosphere-Geochemical or Geophysiological?" Origins Life Evol Biosphere. **24**:435–450. doi:10.1007/BF01582019.

Supplementary data: available at https://doi.org/10.32388/HX4713.3

Declarations

Funding: No specific funding was received for this work.

Potential competing interests: No potential competing interests to declare.